# A macroscopic traffic model based on relaxation time

Khan, Z. H., Gulliver, T. A., Imran, W., Khattak, K. S., Altamimi, A. B., & Qazi, A.

2022

Alexandria Engineering Journal (2022) 61, 585–596

HOSTED BY

Alexandria University

Alexandria Engineering Journal

www.elsevier.com/locate/aej
www.sciencedirect.com

# A macroscopic traffic model based on relaxation time

Zawar Hussain Khan [a], Thomas Aaron Gulliver [b], Waheed Imran [c,*], Khurram Shehzad Khattak [d], Ahmed B. Altamimi [e], Azhar Qazi [f]

[a] Department of Electrical Engineering, University of Engineering and Technology, Peshawar, Pakistan
[b] Department of Electrical and Computer Engineering, University of Victoria, PO Box 1700, STN CSC, Victoria, BC V8W 2Y2, Canada
[c] Department of Civil, Architectural and Environmental Engineering, University of Naples, Federico II, Via Claudio 21 Naples, 80124, Italy
[d] Department of Computer System Engineering, University of Engineering and Technology, Peshawar, Pakistan
[e] Department of Computer Science and Software Engineering, University of Hail, Hail, Saudi Arabia
[f] Department of Electrical Engineering, CECOS University, Peshawar, Pakistan

Received 9 March 2020; revised 6 July 2020; accepted 14 June 2021
Available online 03 July 2021

**KEYWORDS**

Macroscopic traffic flow;
Relaxation time;
Zhang model;
Anisotropy;
Hyperbolicity;
FORCE scheme

**Abstract** A macroscopic model based on analogies with Little's Law is proposed. The relaxation time is employed to characterize changes in density. This change is large for a small relaxation time and large interactions between vehicles occur. The relaxation time encompasses driver behavior which includes the time to perceive and process traffic situations and the resulting actions. Thus, it incorporates the perception and reaction time of a driver. The proposed model is evaluated for a transition caused by a bottleneck on a road and is compared with Zhang model. Performance results are presented which show that traffic evolution with the proposed model is more realistic than with the Zhang model.



## 1. Introduction

Accurate traffic characterization is essential to model congestion and other behavior. In this paper, a traffic model based on traffic velocity and density evolution during transitions is proposed. The alignment during transitions is affected by the response of drivers [36]. For a slow response, there are small changes in density and velocity which is typical of intoxicated or old drivers. Conversely, the response is quick with young or inexperienced drivers. Driver response also depends on the

* Corresponding author.
E-mail addresses: zawarkhan@nwfpuet.edu.pk (Z.H. Khan), agulliver@ece.uvic.ca (T.A. Gulliver), waheed.imran@unina.it (W. Imran), khurram@gwu.edu (K.S. Khattak), altamimi.b@uoh.sa (A.B. Altamimi), azhar@cecos.edu.pk (A. Qazi).

Peer review under responsibility of Faculty of Engineering, Alexandria University.

https://doi.org/10.1016/j.aej.2021.06.042

traffic flow. It is slower in free flow traffic than in congestion which has more interactions between vehicles. Thus, a traffic model should consider driver response.

Traffic characterization can be based on microscopic and macroscopic vehicle behavior [14]. The microscopic approach considers individual vehicle spatial and temporal movements and their interactions. Microscopic models have been developed based on the stochastic headway, and traffic density and flow. Traffic density is the number of vehicles per unit distance, while flow is the product of density and velocity. Macroscopic models consider cumulative traffic behavior based on velocity, density, and flow. Macroscopic traffic characterization is simple [5] and has low computational cost [15]. Thus, macroscopic traffic characterization is considered in this paper.

Lighthill, Whitham and Richards proposed the first macroscopic traffic model which is known as the LWR model [25,28] and can be expressed as

$$\rho_t + (\rho v)_x = 0. \tag{1}$$

where $\rho$ is the density, $v$ is the velocity, and $\rho v$ is the flow. The subscript $t$ denotes temporal change while the subscript $x$ denotes spatial change. This is one of the simplest macroscopic models that have been proposed. With this model, traffic is conserved on an ideal long road with no exits or entrances. This model ignores large changes in flow and small changes in flow occur instantaneously. Further, driver behavior is not considered.

The Payne-Witham (PW) model improves on the LWR model by including driver behavior [33,31]. This model has two equations. The first is based on vehicle conservation and is given by (1). Driver behavior is characterized by the anticipation term in the second equation. Anticipation is driver presumption of forward changes in traffic. The traffic changes due to velocity are characterized by a relaxation term in this equation. The relaxation time $\tau$ is the time required for traffic velocity alignment. The second equation in the PW model is given by [15]

$$v_t + vv_x + \frac{C_0^2}{\rho}\rho_x = \frac{1}{\tau}(v(\rho) - v), \tag{2}$$

where $C_0$ is a constant which characterizes driver behavior with units m/s [20]. The anticipation term is $\frac{C_0}{\rho}\rho_x$ and the relaxation term is $\frac{1}{\tau}(v(\rho) - v)$ [5]. The anticipation term characterizes changes in flow due to a stimuli and the relaxation term characterizes changes in velocity. Traffic alignment occurs based on the equilibrium velocity distribution $v(\rho)$. The PW model assumes that drivers have similar behavior for all road conditions and only small changes in velocity and density occur [3]. As a consequence, the alignment due to a transition [7] is uniform which can result in abrupt changes in traffic over short distances [32].

Several approaches have been considered to address the deficiencies of the PW model. Ross [27] improved the PW model by removing the anticipation term so that driver presumption is ignored [24]. This model cannot characterize traffic flow when there are large changes or congestion. Michaloupolos [22] proposed a model based on road conditions and traffic flow. However, this model has constant parameters which can produce unrealistic traffic behavior. Traffic variables are required which are based on anticipation and relaxation to realistically characterize traffic evolution. Higher order derivatives of the density [2] and velocity [34] have been considered to achieve this goal. Unfortunately, these terms are diffusive and so reduce the effects of large changes. Further, traffic alignment must be based on driver presumption. The second derivative of velocity has been employed to characterize large changes in the PW model [17], but this causes stop and go traffic which is unrealistic.

Traffic flow is influenced by forward traffic conditions but this is neglected in the PW model [3]. As a consequence, Aw and Rascle [1] and Zhang [45,37] developed traffic models which consider these conditions. Aw and Rascle characterized the spatial changes in flow as a monotonic increasing function of density. As a consequence, large changes in acceleration occur with a large forward density which is unrealistic. Zhang employed a speed constant which is the gradient of flow with respect to density, but this ignores driver response. Spatial changes in traffic occur based on changes in the equilibrium velocity distribution with respect to the density. This model considers ideal behavior due to changes in traffic, but a driver requires time to take action. Further, it is assumed that there are only small changes in traffic. Significant vehicle interactions occur at exits, entrances and intersections which can produce large changes in traffic. The first equation of the Zhang model is the same as the LWR model while the second equation is

$$v_t + vv_x + \rho(v\prime(\rho))^2\rho_x = \frac{1}{\tau}(v(\rho) - v). \tag{3}$$

The anticipation term $\rho(v\prime(\rho))^2$ is based only on changes in the equilibrium velocity [46] and ignores the time required by a driver to react.

In this paper, a new traffic model is developed based on analogies with Little's Law [20]. This law specifies the average number of items in a queue as a function of the processing time and arrival rate. The number of items is analogous to the traffic density. During congestion, the density is high and the velocity low while in free flow, the density is low and the velocity can be high. The processing time is analogous to the relaxation time which is used here to characterize driver response. This is the time taken to perceive and process the traffic situation and take action. The arrival rate is analogous to the traffic velocity. Traffic is quicker in free flow traffic compared to in congestion so the arrival rate will be higher. The proposed model has an anticipation term which is based on the relaxation time and traffic density. Conversely, the anticipation term in the Zhang model [32] only considers changes in the equilibrium velocity. This is suitable for low density traffic where the interactions between vehicles are negligible. However, during congestion traffic alignment depends on driver response which can be characterized by the relaxation time.

The proposed and Zhang models are evaluated on a circular road with a transition caused by an inactive bottleneck. An inactive bottleneck results from a higher density ahead. The results obtained show that the Zhang model can produce unrealistic spatial and temporal traffic evolution due to the inadequate characterization of driver behavior. Conversely, the proposed model provides a realistic traffic characterization.

The remainder of the paper is organized as follows. The proposed model is presented in Section II. In Section III, the first order centered (FORCE) technique [15] is used to characterize the proposed and Zhang models. The evaluation of these

model is given in Section IV, and finally some concluding remarks are given in Section V.

## 2. Proposed Model

The waiting and processing times are important performance measures for businesses. According to Little's Law, the number of items processed in a queue is based on the arrival rate and processing time [20] which is given by

$$N = \lambda g, \tag{4}$$

where $N$ is number of items, $\lambda$ is the arrival rate and $g$ is the processing time. Traffic on a road is analogous to items in a queue, the number of items processed is analogous to the temporal change in density, and the arrival rate is analogous to the corresponding change in velocity. Driver response is then the processing time. Based on these analogies, (4) for traffic is

$$\frac{d\rho}{dt} = -\tau \frac{dv}{dt}, \tag{5}$$

where $\tau$ is the relaxation time which is the time required for a driver to perceive a stimulus ahead and then take action. A negative sign is used on the RHS of (5) because the density on a road tends to decrease over time as the traffic moves forward [3]. Traffic leaves an empty space behind on a road when there are no following vehicles [7]. A slow driver takes more time to align to forward conditions so $\tau$ is larger than with an aggressive driver [12]. In convective form, (5) becomes

$$\frac{\partial \rho}{\partial t} + v\frac{\partial \rho}{\partial x} = -\tau\left(\frac{\partial v}{\partial t} + v\frac{\partial v}{\partial x}\right), \tag{6}$$

and rearranging gives

$$\left(\frac{\partial v}{\partial t} + \frac{\partial \rho}{\tau \partial t}\right) + v\left(\frac{\partial v}{\partial x} + \frac{\partial \rho}{\tau \partial x}\right) = 0. \tag{7}$$

This can be expressed as

$$\left(v + \frac{\rho}{\tau}\right)_t + v\left(v + \frac{\rho}{\tau}\right)_x = 0, \tag{8}$$

where the subscripts $x$ and $t$ denote partial derivative with respect to space and time, respectively.

At a transition, traffic aligns to the equilibrium velocity distribution which is characterized by the relaxation term. The flow becomes homogeneous when this distribution is attained. The Greenshields distribution [7,21] is often used for the equilibrium velocity distribution which is given by

$$v(\rho) = v_m\left(1 - \frac{\rho}{\rho_m}\right), \tag{9}$$

where $\rho$ is the average density, $\rho_m$ is the maximum density, and $v_m$ is the maximum velocity (speed limit). This distribution is considered here.

The relaxation term

$$\frac{v(\rho) - v}{\tau},$$

is added to the right hand side of (8) to include traffic behavior during transitions which gives

$$\left(v + \frac{\rho}{\tau}\right)_t + v\left(v + \frac{\rho}{\tau}\right)_x = \frac{v(\rho) - v}{\tau}. \tag{10}$$

In free flow traffic, interactions between vehicles are small so driver behavior has a negligible effect on traffic flow. This results in small changes in velocity at transitions, so we have [17,11,35]

$$\rho_t + (\rho v)_x = 0. \tag{11}$$

Eqs. (10) and (11) constitute the proposed model. In order to evaluate the performance of the proposed and Zhang models, the FORCE scheme is used in the next section to approximate the traffic flow.

## 3. Model Decomposition

In this section, the FORCE scheme [15] is employed to decompose the proposed and Zhang traffic models. It is used to approximate changes in nonlinear systems [12] and is given by

$$G_t + f(G)_x = S(G), \tag{12}$$

where $G$ is the vector of data variables, $f(G)$ is the vector of data variable functions, and $S(G)$ is the source term vector [8]. The subscript $x$ denotes partial derivative with respect to distance, while the subscript $t$ denotes partial derivative with respect to time. Substituting $S(G) = 0$ in (12) gives

$$G_t + f(G)_x = 0, \tag{13}$$

which is a quasilinear form of a nonlinear hyperbolic traffic system. The zero source term indicates that the changes in flow are negligible and there is no egress or ingress to the flow, i.e. the traffic on the road is conserved. $\rho$ and $\rho v$ are data variables in the proposed and Zhang models. The FORCE scheme is employed to approximate a traffic system of the form (13) by providing the flux based on the data variables.

A road of length $x_M$ is divided into $M$ segments of equal size so a road segment has length $\delta x = x_M/M$. The simulation time $t_N$ is divided into $N$ time steps so a time step has duration $\delta t = t_N/N = t_{n+1} - t_n$. $G$ and $f(G)$ are estimated for a segment $(x_i + \frac{\delta x}{2}, x_i - \frac{\delta x}{2})$. The data variables are obtained for each of the $M$ segments.

The FORCE technique [30] can provide accurate solutions for hyperbolic systems such as (12). In the $i$th road segment, the values of the data variables are denoted by $G_i$. The flux for the traffic flow and density at the road segments boundaries is obtained. At time $n$, the flux with the Lax-Friedrichs scheme at the boundary of segments $i$ and $i+1$ is

$$(f^n_{i+\frac{1}{2}}(G^n_i, G^n_{i+1}))^l = \frac{1}{2}\left(f(G^n_i) + f(G^n_{i+1})\right) + \frac{1}{2}\frac{\delta t}{\delta x}\left(G^n_i - G^n_{i+1}\right), \tag{14}$$

where the superscript $l$ denotes the Lax-Friedrichs scheme. For road segments $i$ and $i+1$, $f(G^n_{i+1})$ and $f(G^n_i)$ denote the data variable functions at time $n$. The data variables $G^n_{i+\frac{1}{2}}$ at the segments boundaries obtained with the Richtmyer scheme are then [26]

$$G^n_{i+\frac{1}{2}} = \frac{1}{2}\left(G^n_i + G^n_{i+1}\right) + \frac{1}{2}\frac{\delta t}{\delta x}\left(f(G^n_i) - f(G^n_{i+1})\right), \tag{15}$$

and the corresponding flux can be approximated as

$$(f^n_{i+\frac{1}{2}}(G^n_i, G^n_{i+1}))^r = f(G^n_{i+\frac{1}{2}}), \tag{16}$$

where the superscript $r$ denotes the Richtmyer scheme. The flux at the segment boundaries is obtained by averaging (14) and (16) which gives

$$f_i^{n+1} = \frac{1}{2}\left((f_{i+\frac{1}{2}}^n)^r + (f_{i+\frac{1}{2}}^n)^l\right). \tag{17}$$

This is an approximation of the change in traffic flow and density without considering the source term. The source term in (10) is

$$S(G_i^n) = \rho_i^n\left(\frac{v(\rho_i^n) - v_i^n}{\tau}\right). \tag{18}$$

This term is included to obtain the updated data variables as

$$G_i^{n+1} = G_i^n - \frac{\delta t}{\delta x}\left(f_{i+\frac{1}{2}}^n - f_{i-\frac{1}{2}}^n\right) + \delta t S(G_i^n). \tag{19}$$

$G$ and $f(G)$ are now derived from the conserved form of the models. For the proposed model, let $P(\rho) = \frac{\rho}{\tau}$ and $B = \rho(v + P(\rho))$ so that (11) becomes

$$\rho_t + (B - \rho P(\rho))_x = 0, \tag{20}$$

and (10) is

$$B_t + \left(\frac{B^2}{\rho} - BP(\rho)\right)_x = \frac{v(\rho) - v}{\tau}. \tag{21}$$

Since the source term is zero, this gives

$$B_t + \left(\frac{B^2}{\rho} - BP(\rho)\right)_x = 0. \tag{22}$$

In quasilinear form, this is

$$G = \begin{pmatrix}\rho\\ B\end{pmatrix}, f(G) = \begin{pmatrix}f_1\\ f_2\end{pmatrix} = \begin{pmatrix}B - \rho P(\rho)\\ \frac{B^2}{\rho} - BP(\rho)\end{pmatrix} \text{and} S(G) = \begin{pmatrix}0\\ 0\end{pmatrix}, \tag{23}$$

The Jacobian matrix $A(G) = \frac{\partial f(G)}{\partial G}$ obtained from (23) is

$$A(G) = \begin{pmatrix}-2P & 1\\ -\frac{B^2}{\rho^2} - \frac{P(\rho)B}{\rho} & \frac{2B}{\rho} - P(\rho)\end{pmatrix}. \tag{24}$$

The eigenvalues of (24) are obtained from

$$|A(G) - \lambda I| = \begin{vmatrix}-2P - \lambda & 1\\ -\frac{B^2}{\rho^2} - \frac{P(\rho)B}{\rho} & \frac{2B}{\rho} - P(\rho) - \lambda\end{vmatrix} = 0, \tag{25}$$

which gives

$$\lambda^2 + \left(3P(\rho) - \frac{2B}{\rho}\right)\lambda + \frac{B^2}{\rho^2} + \frac{P(\rho)B}{\rho} - 4\frac{BP(\rho)}{\rho} + 2P(\rho)^2 = 0, \tag{26}$$

so

$$\begin{aligned}\lambda_{1,2} &= \frac{-\left(3P(\rho) - \frac{2B}{\rho}\right) \pm P(\rho)}{2},\\ &= \frac{-(3P(\rho) - 2(v + P(\rho))) \pm P(\rho)}{2},\end{aligned} \tag{27}$$

$$\lambda_1 = \frac{2v - P(\rho) + P(\rho)}{2} = v \quad \text{and}$$
$$\lambda_2 = \frac{2v - P(\rho) - P(\rho)}{2} = v - P(\rho).$$

The proposed model is strictly hyperbolic as the eigenvalues are distinct and real. Thus, the rate of change in the flow is either at or below the average velocity and traffic changes occur due to changes in the relaxation time and density.

The Zhang model in conserved form [23] is

$$\rho_t + (\rho v)_x = 0, \tag{29}$$

$$(\rho(v - v(\rho)))_t + (\rho v(v - v(\rho)))_x = \frac{v(\rho) - v}{\tau}. \tag{30}$$

Let $\gamma = \rho(v - v(\rho))$ so that (29) becomes

$$\rho_t + (\gamma + \rho v(\rho))_x = 0, \tag{31}$$

and (30) is

$$\gamma_t + \left(\frac{\gamma^2}{\rho} + \gamma v(\rho)\right)_x = \frac{v(\rho) - v}{\tau}. \tag{32}$$

From (31) and (32), the quasilinear form is

$$G = \begin{pmatrix}\rho\\ \gamma\end{pmatrix}, f(G) = \begin{pmatrix}f_1\\ f_2\end{pmatrix} = \begin{pmatrix}\gamma + \rho v(\rho)\\ \frac{\gamma^2}{\rho} + \gamma v(\rho)\end{pmatrix} \text{and} S(G) = \begin{pmatrix}0\\ 0\end{pmatrix}, \tag{33}$$

$G$ and $f(G)$ are the used in (17) to estimate the traffic evolution with the Zhang model. The corresponding Jacobian matrix is

$$A(G) = \begin{pmatrix}\rho v'(\rho) + v(\rho) & 1\\ -\frac{\gamma^2}{\rho^2} + v'(\rho)\gamma & \frac{2\gamma}{\rho} + v(\rho)\end{pmatrix}. \tag{34}$$

The eigenvalues $\lambda_i$ of (34) are obtained from

$$|A(G) - \lambda I| = \begin{pmatrix}\rho v'(\rho) + v(\rho) - \lambda & 1\\ -\frac{\gamma^2}{\rho^2} + v'(\rho)\gamma & \frac{2\gamma}{\rho} + v(\rho) - \lambda\end{pmatrix} = 0, \tag{35}$$

which gives

$$\lambda_1 = v \quad \text{and} \quad \lambda_2 = v + \rho v'(\rho). \tag{36}$$

This indicates that the change in acceleration depends on the velocity distribution of the forward traffic which is true only for free flow traffic. Driver response is ignored and thus the Zhang model cannot characterize traffic behavior when there is significant vehicle interaction such as in congestion.

## 4. Simulation Results

In this section, the performance of the Zhang and proposed models is evaluated. The simulation parameters are given in Table 1. The road length is $x_M = 1500$ m and the simulation time is $t_N = 10$ s. Traffic on a circular road is represented by periodic boundary conditions [9]. The Greenshields distribution given by (9) is used for the equilibrium velocity distribution. To ensure numerical accuracy, a small value of $\delta x$ is required [12]. Therefore, $\delta x = 15$ m is used here so the road is divided into $M = 100$ equal segments. The CFL condition [19] is employed to ensure stability which gives $\delta t = 0.01$ s for both models. Therefore, the simulation time is divided into $N = 1000$ intervals. The relaxation times employed are 0.1 s, 1 s and 10 s [16] which correspond to aggressive, typical and sluggish drivers, respectively. The initial density distribution for both models is

$$\rho_0 = \begin{cases}0.01, & \text{for} \quad x \leqslant 750;\\ 0.95, & \text{for} \quad x > 750,\end{cases} \tag{37}$$

**Table 1** Simulation Parameters.

| Parameter | Value |
|---|---|
| equilibrium velocity distribution | $v(\rho)$ |
| maximum normalized density | $\rho_m = 1$ |
| relaxation time | $\tau = 0.1, 1.5, 10$ s |
| maximum velocity | $v_m = 33$ m/s |
| road length | $x = 1500$ m |
| time step | $\delta t = 0.01$ s |
| number of time steps | $N = 1000$ |
| road step | $\delta x = 15$ m |
| number of road steps | $M = 100$ |
| simulation time | $t_N = 10$ s |

which corresponds to congestion. The maximum density is set to 95% occupancy and $v_m = 33$ m/s.

The proposed model density evolution on a 1500 m circular road for $\tau = 1.5$ s at 1 s, 5 s and 10 s is given in Fig. 1. This shows that the density becomes smoother over time, as expected. At 1 s, the density is 0.47 at 1 m, 0.01 between 240 m and 560 m, and then increases to 0.95. At 1500 m, the density decreases to 0.52. At 5 s, the density is 0.49 at 1 m and then decreases to 0.02 at 480 m. At 1070 m, it is 0.94 and then decreases to 0.50 at 1500 m. At 10 s, the density is 0.50 at 1 m, and then decreases to 0.10 at 520 m. It is 0.87 at 1040 m and 0.50 at 1500 m. The corresponding velocity evolution is given in Fig. 2. At 1 s, the velocity is 9.9 m/s at 1 m and is 31.6 m/s between 240 m and 560 m. It then decreases to 1.7 m/s, is approximately constant until 1280 m, and then increases to 8.27 m/s at 1500 m. At 5 s, the velocity is 14.9 m/s at 1 m and increases to 31.4 m/s at 480 m. At 1070 m, it is 2.1 m/s and then increases to 14.3 m/s at 1500 m. At 10 s, the velocity is 15.8 m/s at 1 m, increases to 29.3 m/s at 520 m, and is 4.4 m/s at 1040 m. It is 15.5 m/s at 1500 m. Thus, the velocity becomes smoother over time. Figs. 1 and 2 indicate an inverse relationship between density and velocity.

The density evolution with the Zhang model for $\tau = 1.5$ s at 1 s, 5 s and 10 s on a 1500 m circular road is given in Fig. 3. At 1 s, the density is 0.45 at 1 m and 0.01 between 300 m and 580 m. It is 0.95 between 960 m and 1280 m and decreases to 0.50 at 1500 m. At 5 s, the density is 0.46 at 1 m and decreases to 0.06 at 560 m. It increases to 0.95 at 950 and is 0.50 at 1500 m. At 10 s, the density is 0.46 at 1 m and decreases to 0.16 at 590 m. It is 0.86 at 920 m and 0.50 at 1500 m. The corresponding velocity evolution is given in Fig. 4. At 1 s, the velocity is 12.4 m/s at 1 m and increases to 65.8 m/s at 210 m. Between 300 m and 580 m, it varies between 39.4 m/s and 27.7 m/s. the velocity is 1.6 m/s between 960 m and 1280 m and then increases to 10.7 m/s at 1500 m. At 5 s, the velocity is 15.3 m/s

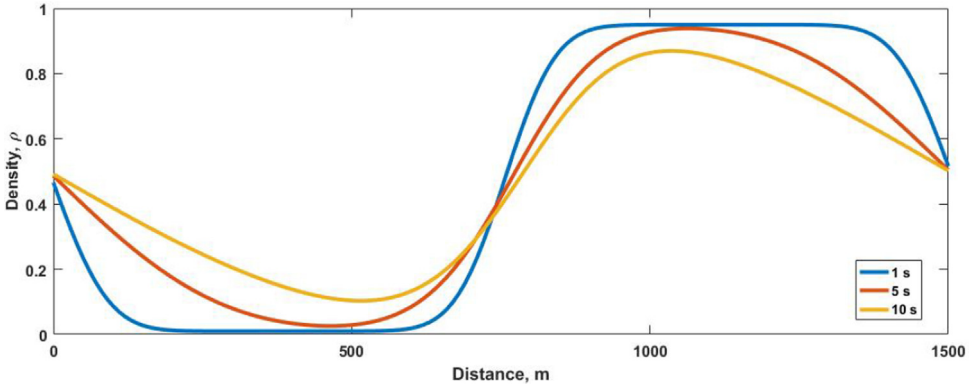


**Fig. 1** The density with the proposed model on a 1500 m circular road for $\tau = 1.5$ s at 1 s, 5 s and 10 s.

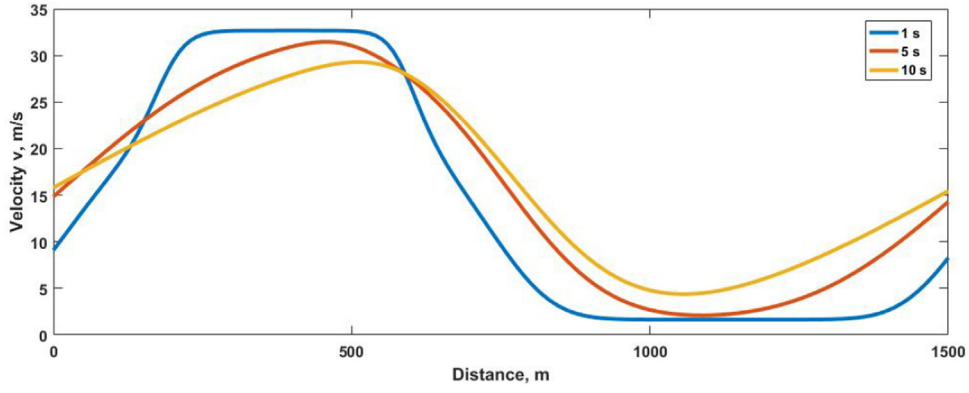


**Fig. 2** The velocity with the proposed model on a 1500 m circular road for $\tau = 1.5$ s at 1 s, 5 s and 10 s.

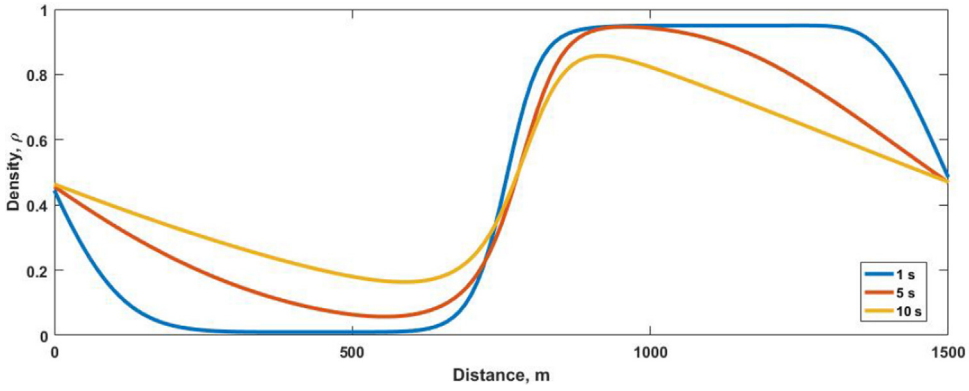


**Fig. 3** The density with the Zhang mode on a 1500 m circular road for $\tau = 1.5$ s at 1 s, 5 s and 10 s.

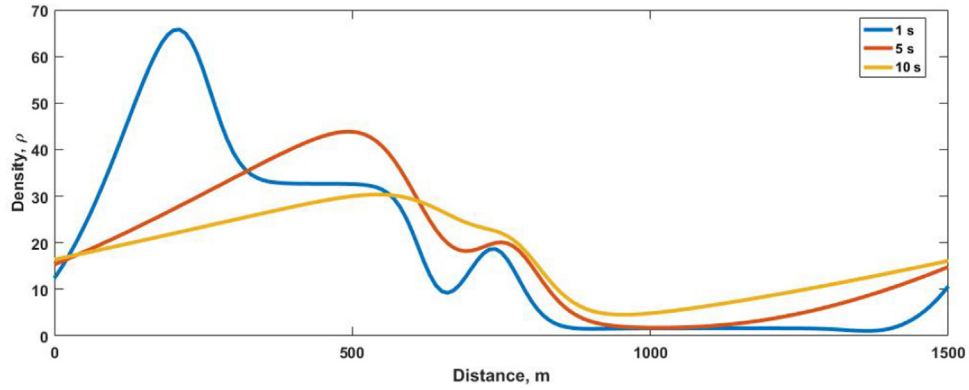


**Fig. 4** The velocity with the Zhang model on a 1500 m circular road for $\tau = 1.5$ s at 1 s, 5 s and 10 s.

at 1 m and increases to 39.4 m/s at 560 m. It decreases to 2.0 m/s at 950 m and then increases to 14.8 m/s at 1500 m. At 10 s, the velocity is 16.4 m/s at 1 m and increases to 29.7 m/s at 590 m. It is 4.9 m/s at 920 m and 16.1 m/s at 1500 m. These results show that the velocity with the Zhang model exceeds the maximum of 33 m/s which is not realistic.

The velocity evolution with the proposed model on a length 1500 m circular road with $\tau = 1.5$ s for 10 s is given in Fig. 5. This shows that the velocity stays within the maximum of 33 m/s and minimum of 0 m/s, and becomes smooth over time. The corresponding results with the Zhang model are given in Fig. 6. In this case, the velocity reaches 65.9 m/s which is not realistic.

The density evolution with the proposed model for $\tau = 0.1$ s on a 1500 m circular road at 1 s, 5 s and 10 s is shown in Fig. 7. At 1 s, the density is 0.51 at 1 m and 0.01 between 240 m and 560 m. It increases to 0.95 at 980 m and is 0.60 at 1500 m. At 5 s, the density is 0.60 at 1 m and decreases to 0.02 at 520 m. It is 0.93 at 1100 m and decreases to 0.60 at 1500 m. At 10 s, the density is 0.60 at 1 m and 0.10 at 590 m. It is 0.85 at 1140 m and then 0.60 at 1500 m. The corresponding velocity evolution is shown in Fig. 8. At 1 s, the velocity is 15.9 m/s at 1 m and is

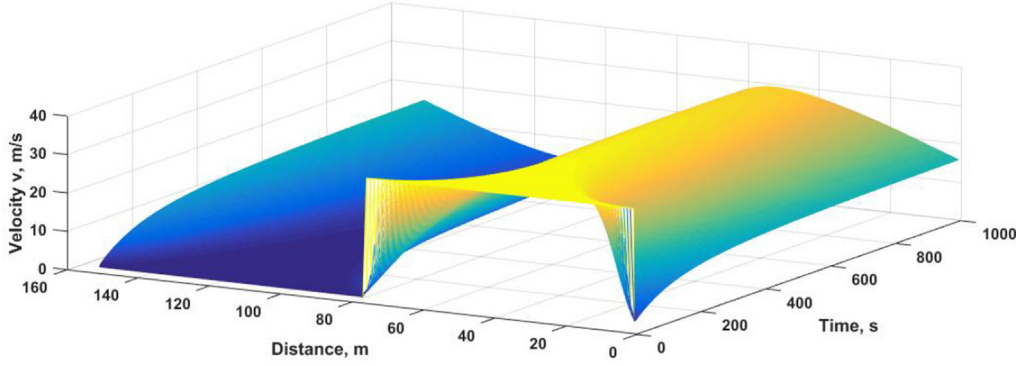


**Fig. 5** The velocity with the proposed model on a 1500 m circular road for 10 s with $\tau = 1.5$ s.

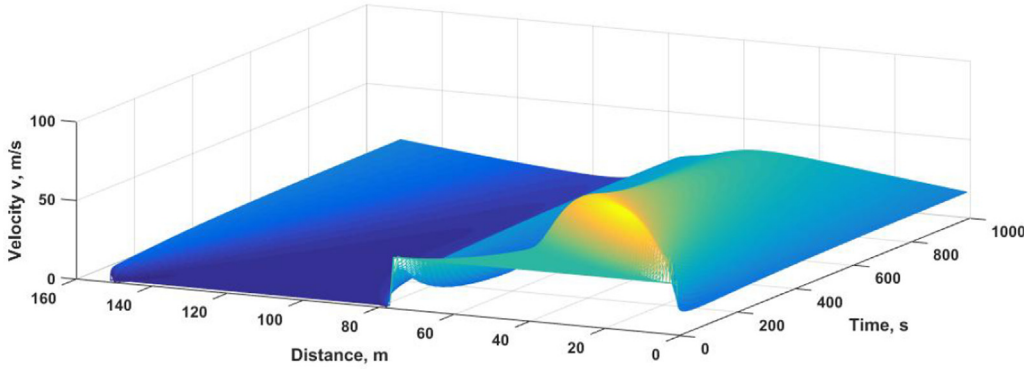


**Fig. 6** The velocity with the Zhang model on a 1500 m circular road for 10 s with $\tau = 1.5$ s.

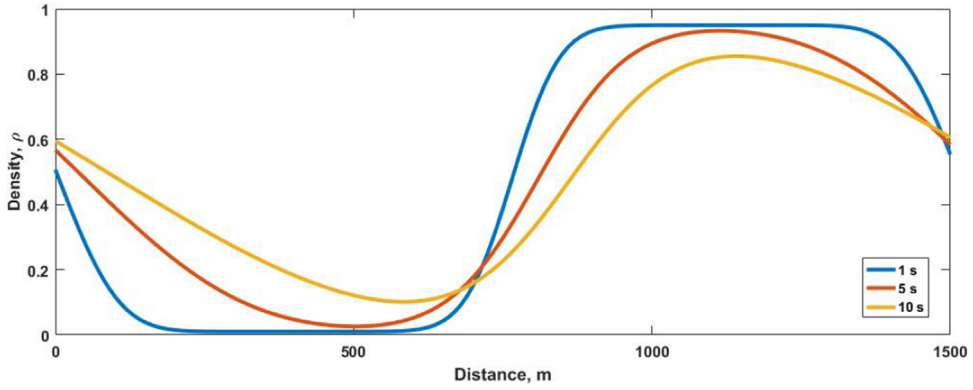


**Fig. 7** The density with the proposed model on a 1500 m circular road for $\tau = 0.1$ s at 1 s, 5 s and 10 s.

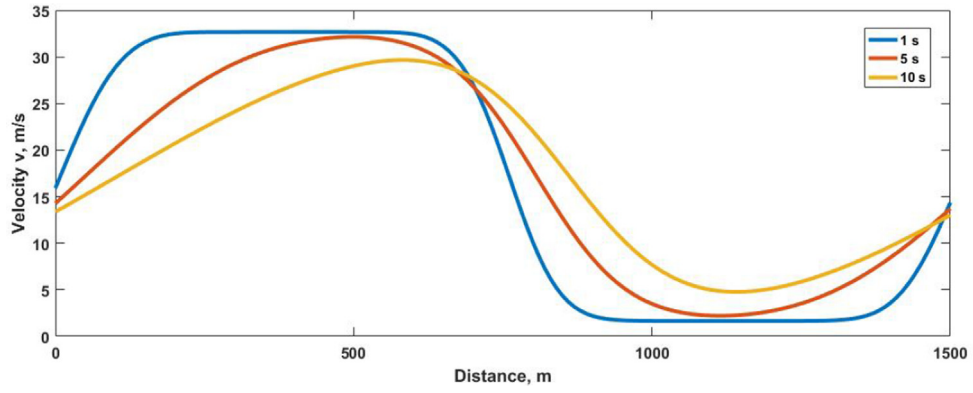


**Fig. 8** The velocity with the proposed model on a 1500 m circular road for $\tau = 0.1$ s at 1 s, 5 s and 10 s.

32.7 m/s between 240 m and 560 m. It decreases to 1.7 m/s at 980 m, stays approximately constant until 1280 m, and then increases to 14.8 m/s at 1500 m. At 5 s, the velocity is 14.8 m/s at 1 m and increases to 32.2 m/s at 500 m. It decreases to 2.2 m/s at 1100 m and then increases to 13.7 m/s at 1500 m. At 10 s, the velocity is 13.8 m/s at 1 m and increases to 29.7 m/s at 590 m. It is 4.8 m/s at 1140 m and 13.0 m/s at 1500 m.

The density evolution with the Zhang model on a 1500 m circular road for $\tau = 0.1$ s at 1 s, 5 s and 10 s is shown in Fig. 9. At 1 s, the density is 0.50 at 1 m and is approximately 0.01 between 270 m and 590 m. It is 0.95 between 920 m and 1260 m and decreases to 0.50 at 1500 m. At 5 s, the density is 0.50 at 1 m and decreases to 0.04 at 600 m. It increases to 0.93 at 940 m and is 0.50 at 1500 m. At 10 s, the density is 0.50 at 1 m and decreases to 0.16 at 620 m. It is 0.80 at 940 m and 0.50 at 1500 m. The corresponding velocity evolution is shown in Fig. 10. At 1 s, the velocity is 17.2 m/s at 1 m and increases to 37.3 m/s at 190 m. Between 270 m and 590 m, it is 32.6 m/s and between 920 m and 1260 m it is 1.7 m/s. It then increases to 15.8 m/s at 1500 m. At 5 s, the velocity is 16.9 m/s at 1 m and increases to 33.0 m/s at 520 m. At

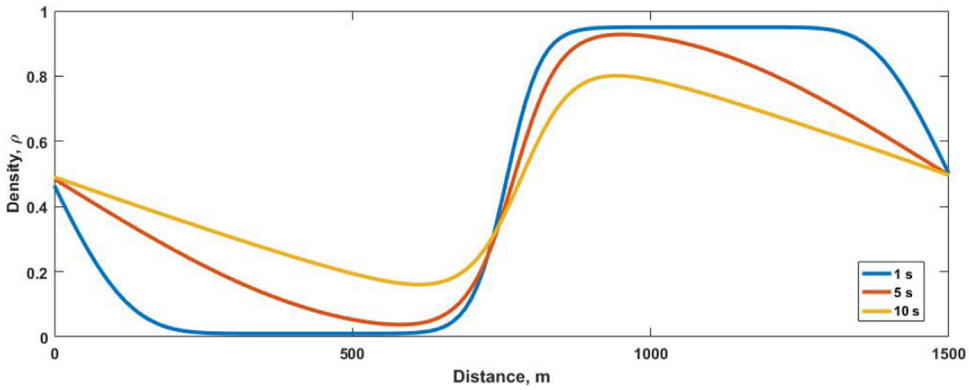


**Fig. 9** The density with the Zhang model on a 1500 m circular road for $\tau = 0.1$ s at 1 s, 5 s and 10 s.

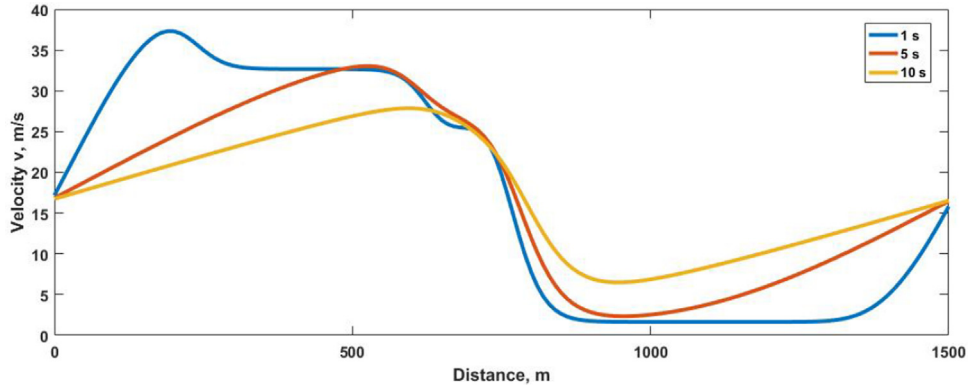


**Fig. 10** The velocity with the Zhang model on a 1500 m circular road for $\tau = 0.1$ s at 1 s, 5 s and 10 s.

600 m it is 30.9 m/s, decreases to 2.4 m/s at 940 m, and is 16.5 m/s at 1500 m. At 10 s, the velocity is 16.8 m/s at 1 m and increases to 27.7 m/s at 620 m. It is 6.5 m/s at 940 m and 16.5 m/s at 1500 m.

The velocity evolution with the proposed model on a 1500 m circular road for 10 s and $\tau = 0.1$ s is given in Fig. 11. The corresponding results with the Zhang model are given in Fig. 12. This shows that the velocity becomes smooth over time, as expected. Further, the variations in velocity with the proposed model are small compared to the Zhang model, The velocity with the proposed model is within the range 0 m/s to 33 m/s, but the velocity with the Zhang model goes above the maximum to 37.3 m/s. Thus, the Zhang model produces unrealistic behavior.

The density evolution with the proposed model on a 1500 m circular road for $\tau = 10$ s at 1 s, 5 s and 10 s is shown in Fig. 13. At 1 s, the density is 0.46 at 1 m and 0.01 between 200 m and 550 m. It increases to 0.95 at 970 and is 0.50 at 1500 m. At 5 s, the density is 0.48 at 1 m and decreases to 0.02 at 400 m. It is 0.93 at 1120 m and then decreases to

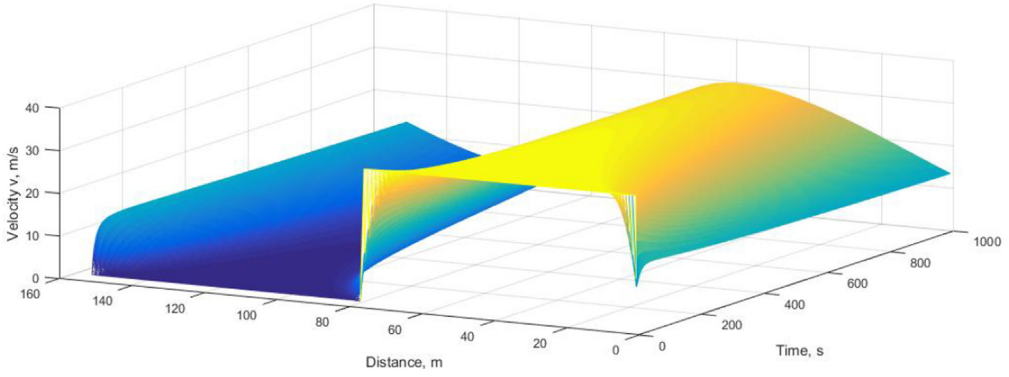


**Fig. 11** The velocity with the proposed model on a 1500 m circular road for 10 s and $\tau = 0.1$ s.

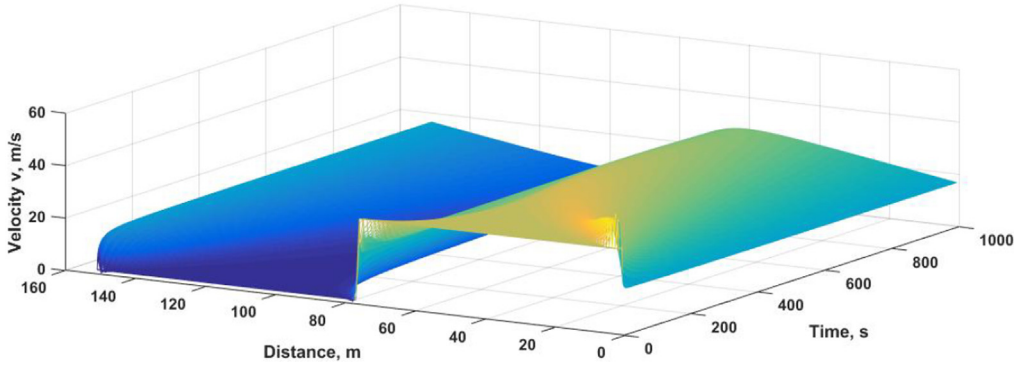


**Fig. 12** The velocity with the Zhang model on a 1500 m circular road for 10 s and $\tau = 0.1$ s.

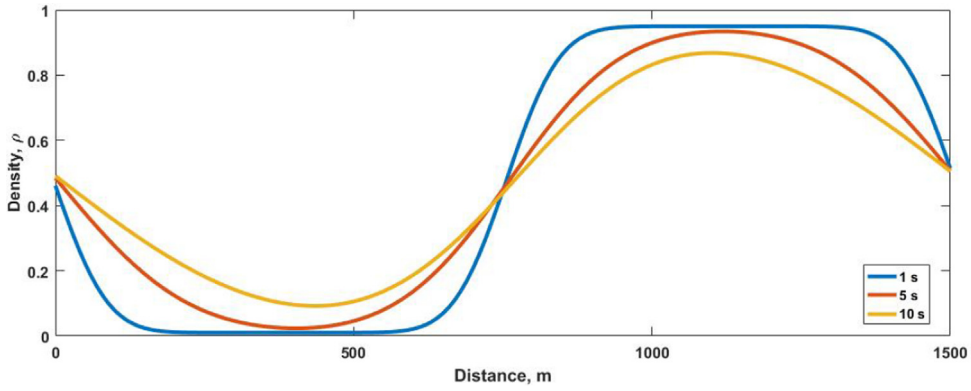


**Fig. 13** The density with the proposed model on a 1500 m circular road for $\tau = 10$ s at 1 s, 5 s and 10 s.

0.50 at 1500 m. At 10 s, the density is 0.49 at 1 m and decreases to 0.09 at 450 m. It is 0.87 at 1100 m and 0.50 at 1500 m.

The velocity evolution with the proposed model on a length 1500 m circular road for $\tau = 10$ s at 1 s, 5 s and 10 s is shown in Fig. 14. At 1 s, the velocity is 3.0 m/s at 1 m. From 290 m to 490 m it is 32.6 m/s and between 970 m and 1300 m it is 1.7 m/s. The velocity is 2.8 m/s at 1500 m. At 5 s, the velocity is 5.8 m/s at 1 m and decreases to 19.3 m/s at 400 m. It is 1.8 m/s at 1120 m and then increases to 5.6 m/s at 1500 m. At 10 s, the velocity is 8.3 m/s at 1 m and increases to 17.7 m/s at 450 m. It is 3.2 m/s at 1100 m and 8.1 m/s at 1500 m.

The density evolution with the Zhang model at 1 s, 5 s and 10 s on a 1500 m circular road for $\tau = 10$ s is shown in Fig. 15. At 1 s, the density is 0.44 at 1 m. It is 0.01 between 320 m and 580 m and 0.95 between 990 m and 1300 m. The density then decreases to 0.48 at 1500 m. At 5 s, the density is 0.43 at 1 m, decreases to 0.05 at 540 m, increases to 0.95 at 960 m, and then decreases to 0.44 at 1500 m. At 10 s, the density is 0.42 at 1 m and then decreases to 0.12 at 560 m. It is 0.99 at 920 m and 0.43 at 1500 m. The corresponding velocity evolution is shown in Fig. 16. At 1 s, the velocity is 8.7 m/s at 1 m and increases to 80.9 m/s at 290 m. Between 320 m and 580 m, it changes from

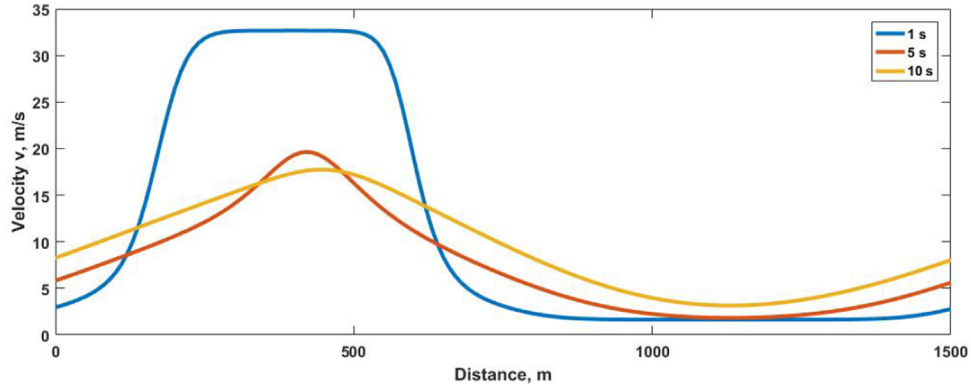


**Fig. 14** The velocity with the proposed model on a 1500 m circular road for $\tau = 10$ s at 1 s, 5 s and 10 s.

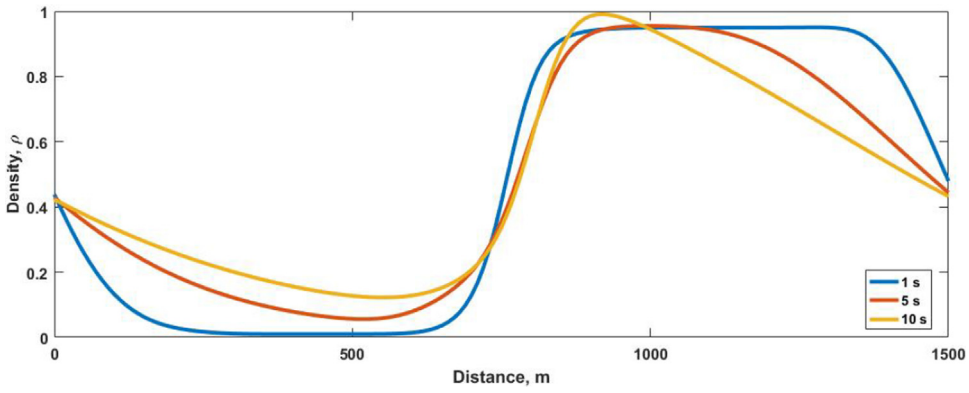


**Fig. 15** The density with the Zhang model on a 1500 m circular road for $\tau = 10$ s at 1 s, 5 s and 10 s.

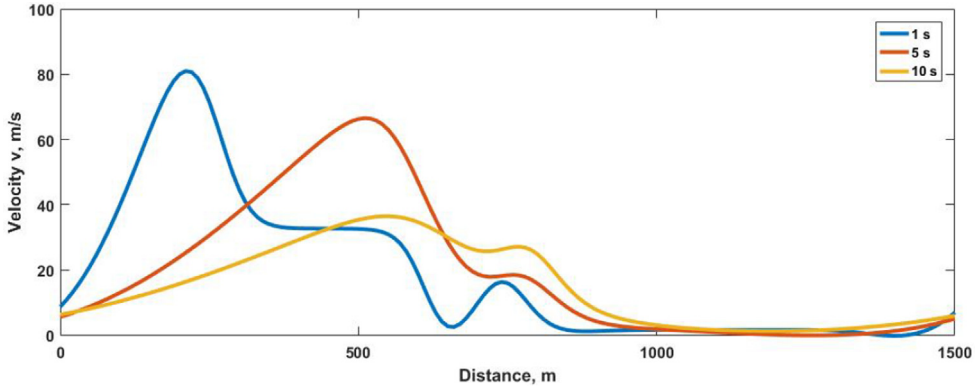


**Fig. 16** The velocity with the Zhang model on a 1500 m circular road for $\tau = 10$ s at 1 s, 5 s and 10 s.

38.2 m/s to 25.7 m/s. The velocity is 1.6 m/s between 990 m and 1300 m and then increases to 6.9 m/s at 1500 m. At 5 s, the velocity is 5.6 m/s at 1 m and increases to 64.6 m/s at 540 m. It then decreases to 2.3 m/s at 960 m and is 5.0 m/s at 1500 m. At 10 s, the velocity is 6.3 m/s at 1 m and increases to 36.5 m/s at 560 m. It is 6.2 m/s at 920 m and 5.9 m/s at 1500 m.

The velocity evolution with the proposed model on a 1500 m circular road for 10 s and $\tau = 10$ s is given in Fig. 17. The corresponding results for the Zhang model are given in Fig. 18. These results show that the velocity becomes smooth over time. However, the velocity with the proposed model stays within the maximum and minimum values whereas the velocity with the Zhang model reaches 80.9 m/s, which is impossible.

The velocity evolution with the proposed model for $\tau = 1.5$ s, 0.1 s and 10 s is shown in Figs. 5, 11 and 17, respectively. With $\tau = 1.5$ s, the variations in velocity are larger than with $\tau = 10$ s, which represents a sluggish driver, while with $\tau = 0.1$ s, which represents an aggressive driver, the variations

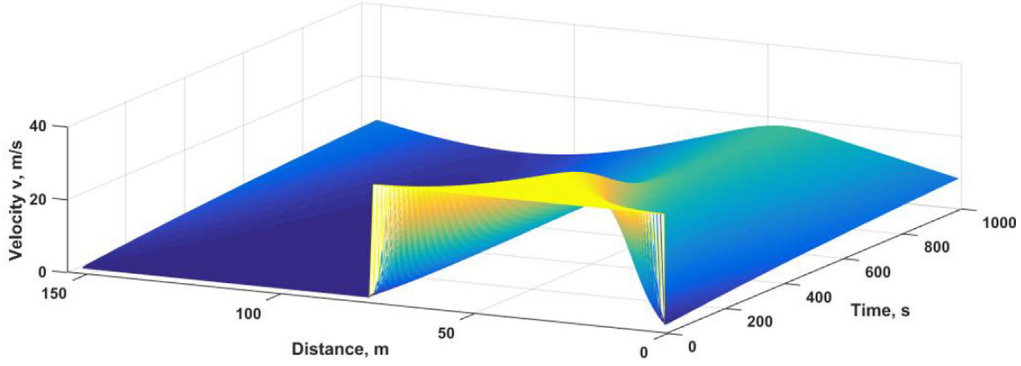


**Fig. 17** The velocity with the proposed model on a 1500 m circular road for 10 s and $\tau = 10$ s.

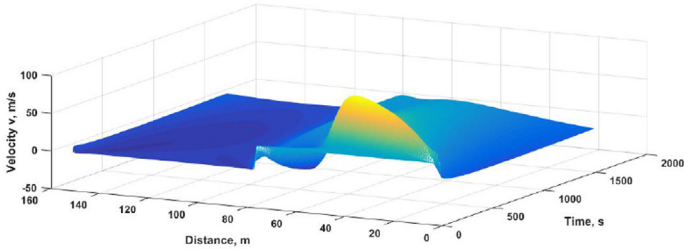


**Fig. 18** The velocity with the Zhang model on a 1500 m circular road for 10 s and $\tau = 10$ s.

are even greater. However, the velocity is always between the maximum and minimum values. The corresponding results for the Zhang model are given in Figs. 6, 12 and 18, respectively. The variations in velocity are larger with a sluggish driver ($\tau = 10$ s) than with a typical ($\tau = 1.5$ s) or aggressive ($\tau = 0.1$ s) driver, which is not realistic [29]. The highest velocity is 65.9 m/s with $\tau = 1.5$ s, 37.3 m/s with $\tau = 0.1$ s and 80.9 m/s with $\tau = 10$ s, which exceed the maximum of 33 m/s. The changes in density with the Zhang model are small for all values of $\tau$ as shown in Figs. 3, 9 and 15. The corresponding changes are greater with the proposed model but are smooth as shown in Figs. 1, 7 and 13.

## 5. Conclusion

A new macroscopic traffic model was proposed which is based on analogies with Little's Law. The relaxation time is used to characterize driver response. In the Zhang model, this response is characterized by the change in velocity due to forward conditions. The proposed model was compared with the Zhang model for an inactive bottleneck with three different relaxation times, $\tau = 0.1, 1.5$ and 10 s, which correspond to aggressive, typical and sluggish drivers, respectively. It was shown that the behavior with the proposed model is better than that with the Zhang model. The velocities stayted within the minimum and maximum limits, and the density and velocity became smooth over time. Conversely, the Zhang model produced velocities above the maximum for all relaxation times which is not realistic. This is because the changes in velocity with this model are not based on the changes in density so large variations in velocity can occur for small changes in density.

## Declaration of Competing Interests

The authors declare that they have no known competing financial interests or personal relationships that could have appeared to influence the work reported in this paper.

## Acknowledgments

This project was supported by the Higher Education Commission, Pakistan, under the establishment of the National Center of Big Data and Cloud Computing at the University of Engineering and Technology, Peshawar, Pakistan.

## References

[1] A. Aw, M. Rascle, Resurrection of "second order" models of traffic flow, SIAM J. Appl. Math. 60 (3) (2000) 916–938.
[2] P. Berg, A. Mason, A. Woods, Continuum approach to car-following models, Phys. Rev. E 61 (2) (2000) 1056–1066.
[3] C.F. Daganzo, Requiem for second-order fluid approximations of traffic flow, Transpn. Res. B 29 (4) (1995) 277–286.
[4] B.D. Greenshields, A study in highway capacity, Proc. Highway Res. Board 14 (1935) 448–477.
[5] W. Imran, Z.H. Khan, T.A. Gulliver, K.S. Khattak, H. Nasir, A macroscopic traffic model for heterogeneous flow, Chin. J. Phys. 63 (2020) 419–435.
[6] P. Kachroo, S.J. All-Nasur, S.A. Wadoo, A. Shende, Pedestrian Dynamics - Feedback Control of Crowd Evacuation, Springer-Verlag, Berlin, 2008.
[7] Z.H. Khan, Traffic flow modelling for intelligent transportation systems, Ph.D. dissertation, Dept. Electrical & Computer Eng., University of Victoria, Victoria, BC, 2016.
[8] Z.H. Khan, T.A. Gulliver, A macroscopic traffic model based on anticipation, Arabian J. Sci. Eng. 44 (2019) 5151–5163.
[9] Z.H. Khan, T.A. Gulliver, H. Nasir, A. Rehman, K. Shahzada, A macroscopic traffic model based on driver physiological response, J. Eng. Math. 115 (2019) 21–41.
[10] Z.H. Khan, T.A. Gulliver, A macroscopic traffic model for traffic flow harmonization, Eur. Transp. Res. Rev. 10 (2018) 30.
[11] Z.H. Khan, S.A.A. Shah, T.A. Gulliver, A macroscopic traffic model based on weather conditions, Chin. Phys. B. 27 (2018) 070202.
[12] Z.H. Khan, T.A. Gulliver, K.S. Khattak, A. Qazi, A macroscopic traffic model based on reaction velocity, Iran. J. Sci. Technol. Trans. Civ. Eng. 44 (1) (2019) 139–150.
[13] Z.H. Khan, W. Imran, S. Azeem, K.S. Khattak, T.A. Gulliver, M.S. Aslam, A macroscopic traffic model based on driver reaction and traffic stimuli, Appli. Sci. 9 (14) (2019) 2848.
[14] Z.H. Khan, T.A. Gulliver, A macroscopic traffic model based on transition velocities, J. Computational Sci. 43 (2020) 101131.
[15] Z.H. Khan, W. Imran, T.A. Gulliver, K.S. Khattak, Z. Wadud, A.N. Khan, An anisotropic traffic model based on driver interaction, IEEE Access 8 (2020) 66799–66812.
[16] A. Kesting, M. Treiber, Calibrating car-following models by using trajectory data, J. Transpn Res. B. 2088 (1) (2008) 148–156.
[17] R.D. Kuhne, Freeway control using a dynamic traffic flow model and vehicle reidentification techniques, Transpn. Res. Rec. 1320 (1991) 251–259.
[18] M.J. Lighthill, J.B. Whitham, On kinematic waves II: A theory of traffic flow on long crowded roads, Proc. R. Soc. London Ser. A. 229 (1178) (1955) 317–345.

[19] LeVeque, R.J., Numerical Methods for Conservation Laws, 2nd. ed., Lectures in Mathematics, ETH Zürich, Birkhäuser Verlag, Basel, Switzerland, 1992.
[20] J.D.C. Little, A proof for the queuing formula: $L = \lambda W$, Oper. Res. 9 (3) (1961) 383–387.
[21] A. Muralidharan, Tools for modeling and control of freeway networks, Ph.D. dissertation, Dept. Mechanical Engineering, Univ. California Berkeley, Berkeley, CA, 2012.
[22] P.G. Michalopoulos, P. Yi, A.S. Lyrintzis, Continuum modelling of traffic dynamics for congested freeways, Transp. Res. B: Methodological 27 (4) (1993) 315–332.
[23] J.V. Morgan, Numerical methods for macrosopic traffic models, Ph.D, dissertation, Dept. Math., Univ, Reading, Berkshire, UK, 2002.
[24] G.F. Newell, Comments on traffic dynamics, Transp. Res. B: Methodological 23 (5) (1989) 386–389.
[25] H.J. Payne, Models of freeway traffic and control, Simulation Council Proc. 1 (1) (1971) 51–61.
[26] R.D. Richtmyer, K.W. Morton, Difference Methods for Initial-value Problems, 2nd ed., Wiley, New York, 1967.
[27] P. Ross, Traffic dynamics, Transp. Res. B: Methodological 22 (6) (1988) 421–435.
[28] P.I. Richards, Shock waves on the highway, Oper. Res. 4 (1) (1956) 42–51.
[29] R. Tscharn, F. Naujoks, A. Neukum, The perceived criticality of different time headways is depending on velocity, Transp. Res. F. 58 (2018) 1043–1052.
[30] E.F. Toro, On Glimm-related schemes for conservation laws, Technical report MMU-9602, Dept. Math. and Physics, Manchester Metropolitan Univ, UK, 1996.
[31] G.B. Whitham, Linear and Nonlinear Waves, Wiley, New York, 1974.
[32] H.M. Zhang, A theory of non-equilibrium traffic flow, Transpn. Res. B 32 (7) (1998) 485–498.
[33] H.M. Zhang, A non-equilibrium traffic model deviod of gas-like behavior, Transpn. Res. B 36 (3) (2002) 275–290.
[34] H. Zhang, Driver memory, traffic viscosity and a viscous vehicular traffic ow model, Transp. Res. B: Methodological 37 (1) (2003) 27–41.
[35] L. Zheng, P.J. Jin, H. Huang, An anisotropic continuum model considering bi-directional information impact, Transpn. Res. B. 75 (2015) 36–37.
[36] L. Zheng, C. Zhu, T. He, S. Liu, Empirical validation of vehicle type-dependent car-following heterogeneity from micro- and macro-viewpoints, Transportmetrica B 7 (1) (2019) 765–787.
[37] L. Zheng, Z. He, T. He, An anisotropic continuum model and its calibration with an improved monkey algorithm, Transportmetrica A 13 (6) (2017) 519–543.